JOURNAL OF COMPUTATIONAL PHYSICS 38, 212–226 (1980)

The Representation of Shock-Like Solutions in an Eulerian Mesh

G. KNORR AND M. MOND

Department of Physics and Astronomy,
The University of Iowa, Iowa City, Iowa 52242

Received December 12, 1978; revised September 13, 1979

Methods are presented for integrating differential equations in conservation form in an Eulerian mesh in the presence of discontinuities and shocks. We make use of the monotonicity property, namely, that a solution is assumed to be monotone between mesh points. Monotonicity is preserved by convective equations and can be rigorously implemented in a code. In more general systems of conservative equations, monotonicity is enforced when interpolating a curve, given on an integer mesh, onto a half-integer mesh. This can be interpreted as introducing a local diffusive term whenever a discontinuity or shock occurs. The integration of a Riemann problem shows that with this method shocks are represented within two zones and contact discontinuities exhibit little diffusion.

1. INTRODUCTION

It is well known that the occurrence of shocks and discontinuities in nonlinear hyperbolic equations causes certain difficulties if these equations are solved numerically [1–3]. On the one hand, one would like to have a higher order scheme—usually second order—in the independent variables which reproduces the smooth parts of the solution with high accuracy. On the other hand, shocks should have a sharp transition and (contact) discontinuities should not rapidly diffuse; both should propagate with the correct speed. When higher order methods are being used, shocks may produce nonphysical oscillations which propagate into the smooth part of the solution. Also, over- and undershooting may occur, if the integration method is not diffusive enough to damp out such effects. But diffusion should be kept at a minimum to maintain a high resolution of the solution.

Several new approaches have been suggested during recent years which cope with this problem. Among those are the following: In the flux-corrected transport (FCT) [4–7], a given density dtsribution is advanced in time according to the continuity equation and diffused so much that all overshooting is avoided. In an antidiffusion stage the diffusion is in part or completely taken out again, however restricted to the condition, so that no new extrema should be created, nor should the antidiffusion stage accentuate already existing extrema.

0021-9991/80/140212–15$02.00/0
Copyright © 1980 by Academic Press, Inc.
All rights of reproduction in any form reserved.

The artificial compression method (ACM) of Harten [8, 9] prevents the smearing of contact discontinuities and improves the resolution of shocks. An equation is solved which differs from the original equation by artificial terms which steepen an existing discontinuity.

The monotonicity principle is discussed by Van Leer [10–12] and others [9]. It makes use of a property of the equation

$$\frac{\partial u}{\partial t} + \frac{\partial}{\partial x} f(u) = 0. \tag{1}$$

If the solution $u(x, t)$ or a part of it is monotone at time t, it will remain so for later times.

Sod [13] has compared these and other methods by solving a Riemann problem. He also gave a more elaborate description of the various methods.

We will describe methods for implementing the monotonicity principle in a simple way for convective equations (1) and for modifying it for systems in conservation form,

$$\frac{\partial}{\partial t}\mathbf{u} + \frac{\partial}{\partial x}\mathbf{F}(\mathbf{u}) = 0, \tag{2}$$

where $\mathbf{u}$ and $\mathbf{F}$ are vectors. The schemes are of second order in Δt and of second or higher order in Δx and preserve the flux. They represent discontinuities and shocks well and are easy to implement.

In Section 2 we discuss the convective equation, in Section 3 the conservative system. Section 4 deals with the treatment of discontinuities for conservative systems and in Section 5 the conclusions are stated.

2. Convective Equations

In this section we consider equations of the type (1). The solution of (1) is given by

$$u(x, t) = u\left(x - \frac{\partial f(u)}{\partial u} t, 0\right). \tag{3}$$

The value of u does not change along a characteristic $dx/dt = \partial/\partial u\, F(u)$, so that the set of function values is constant in time. If $F(u) = au$, where a is a constant, (1) reduces to

$$\frac{\partial}{\partial t} u(x, t) = -a \frac{\partial u}{\partial x}. \tag{4}$$

The solution of (4) can be described as a translation of a profile $u(x, 0)$ at time $t = 0$ moving with velocity a.

Examples of equations of type (1) or (2) are the Vlasov equations, which describe the motion of an incompressible phase space fluid. By splitting, it can be brought exactly into form (4) [14]. Other examples are the continuity equation in incompressible hydrodynamics or isentropic one-dimensional compressible gas dynamics.

In order to find $u(j\Delta x, (n+1)\Delta t) = u_j^{n+1}$ at time level $(n+1)$ if u_j^n is given from Eq. (4) for $a > 0$, we construct the characteristic through point j at time level $(n+1)$ and trace it back to level n. The value of $u^n(x)$ at level n on the characteristic is the desired value of u_j^{n+1}.

Assuming that $0 < \partial/\partial u\, F(u)\, \Delta t/\Delta x = \varepsilon < 1$, we have

$$\text{Min}(u_{j-1}^n, u_j^n) < u_j^{n+1} \leqslant \text{Max}(u_{j-1}^n, u_j^n). \tag{5}$$

This condition is violated only if the profile $u^n(x)$ has an extremum between u_{j-1}^n and u_j^n. We will see later that if inequality (5) is enforced, maxima and minima will be reduced somewhat by this effect. Equation (5) is called the monotonicity condition [12].

All interpolation formulae used to find u_j^{n+1} assume that the values u_j^n are varying smoothly and some kind of Taylor expansion or function fitting is meaningful. These assumptions are justified most of the time but in the neighborhood of shocks it leads to gross over- or undershooting as is shown in Fig. 1. This overshooting creates troubles when a discontinuous solution is represented in an Eulerian mesh.

The overshooting can be eliminated by checking if condition (5) is satisfied after the solution for level $(n+1)$ has been calculated by any kind of convective scheme. From Fig. 1 it is evident that overshooting for cubic interpolating between four adjacent points is only about half as much as for a parabola. We therefore consider the slightly more complicated cubic interpolation formula justified and use it in an upstream difference method. However, the method to be described is applicable to any interpolation scheme.

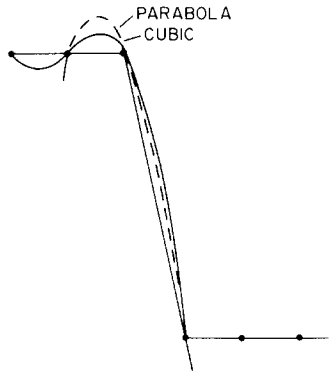

FIG. 1. When a square wave shock is interpolated by a parabola or a cubic, overshooting occurs. The overshooting of the cubic is roughly half as big as that of the parabola.

If condition (5) is not satisfied, we change u_j^{n+1} by the minimum amount into $\tilde{u}_j^{n+1}$ so that (5) is now satisfied for all $\tilde{u}_j^{n+1}$. Inequality (5) can be reformulated in the following way:

$$A_j = S \cdot \text{Max}\{0, \text{Min}((u_j^{n+1} - u_{j-1}^u) \cdot S, |u_j^{n+1} - u_j^n|)\}, \tag{6}$$

where $S = \text{sign}(u_j^{n+1} - u_j^n)$ and the corrected value of u_j^{n+1} is given by

$$\tilde{u}_j^{n+1} = u_j^{n+1} - A_j. \tag{7}$$

The reader can easily convince himself that (6) and (7) produce the desired results. The implementation of (6) and (7) is called the clipping stage. The clipping process (7) destroys flux conservation. We can, however, restore flux conservation if the clipping A_j are added to the values $u_{j\pm r}$, $r = \pm 1, \pm 2, \ldots$, subject to the restraint that no new extrema are created. Let us assume that at mesh point j there is a nonvanishing clipping A_j, u_j has been changed, and therefore $\tilde{u}_j = u_{j-1}$ or u_{j+1}. Assume, for example, $\tilde{u}_j = u_{j-1}$. We do not change u_{j-1} at all but ask if we can add A_j to u_{j+1}. If this is possible without creating a new extremum, we add A_j to u_{j+1}; $\tilde{u}_{j+1} = u_{j+1} + A_j$. If, however, a new extremum would be created, we add only the largest possible fraction of A_j to u_{j+1} such that a new extremum is avoided. Then we ask if the surviving rest of A_j can be added to u_{j+2} and the process is repeated. In this way the whole amount of A_j is distributed to neighboring mesh points and conservation of $\sum_{j=1}^{N} u_j$ is enforced. Two different subroutines were written. In the first, the full process described above was implemented; in the second, only the first two steps were implemented with the provision that the rest of A_j be added to $u_{j\pm 3}$ without checking for overshooting. In the actual runs the two versions gave practically the same results.

A simple illustration is shown in Fig. 2. The details of the advancing of the discontinuity is described in detail in the figure caption. The final result is a shock-like

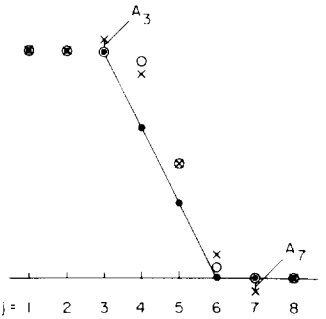

FIG. 2. The figure illustrates how the flux correction works. The shock profile at time n is indicated by solid dots. Advancing Eq. (1) by cubic interpolation with $\varepsilon = v\Delta t/\Delta x$ produces points indicated by crosses. Clearly $j = 3$ and $j = 7$ show over- and underschooting. In the clipping stage the amount A_3 is subtracted from u_3 and A_7 is subtracted from u_7. In the flux-correcting stage A_3 is added to u_4 and A_7 to u_6. The final form is indicated by the circles. Thus the "mass" is conserved, the dissipation is decreased and the scheme is positive definite.

structure described by the circled points, which does not exhibit any overshooting and which is flux conserving.

We used the cubic interpolation scheme to propagate a unit pulse according to (4) with periodic boundary conditions using interpolation, clipping and flux correction for $\varepsilon = a\Delta t/\Delta x = 0.2$. This is exactly the test which Boris and Book used for FCT. The only difference is that Boris and Book used 100 points whereas we use only 50, which is enough to keep the discontinuities well separated from each other. The result is shown in Figs. 3a, b, c for 10, 100 and 800 time steps. The flanks of the discontinuities are represented by 3, 5 or 8 points, respectively. Note that the form of the discontinuity is highly symmetric, which is in contrast to the results of FCT.

When running the square wave test we noticed that the test should say something about the overall quality of the integration scheme. The square wave test consists essentially of straight lines which are exactly represented by any difference scheme. Thus, it is difficult to judge the overall performance of a given code from the square wave test. Consequently we used a sine test, which is a sine wave interrupted by a discontinuity, and repeated the runs. The results are shown in Figs. 4a, b for 0, 10, 100 and 800 time steps, again with $\varepsilon = 0.2$. After 800 time steps the discontinuity has broadened so that it is represented by eight points. Also the amplitude has decreased by about 6%. This is a consequence of enforcing (5) even in places where there is an

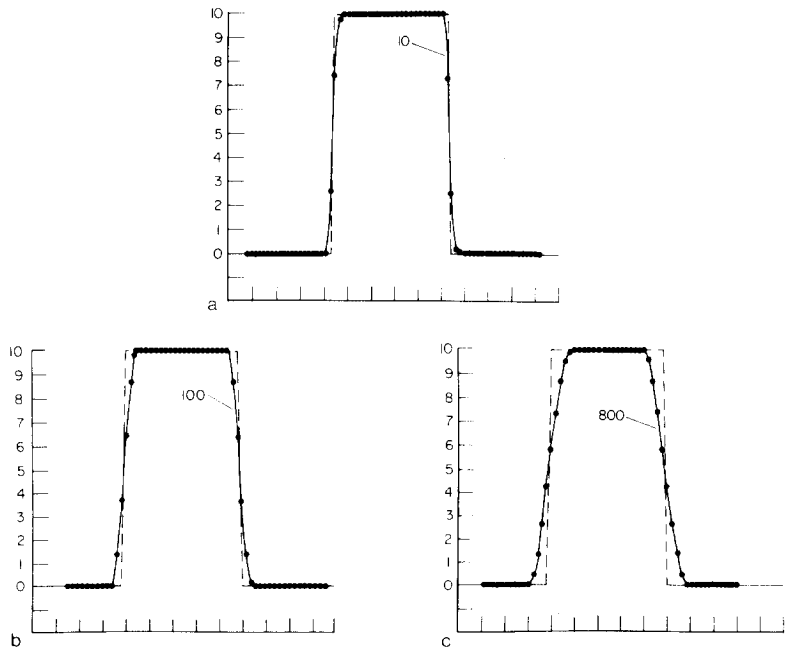

FIG. 3. Propagation of a square wave on a circle according to Eq. (1). The time step is such that $\varepsilon = v\Delta t/\Delta x = 0.2$. Cubic interpolation, clipping and flux correction were implemented. The dashed line indicates the analytical solutions. (a) After 10 time steps, (b) after 100 time steps, (c) after 800 time steps.

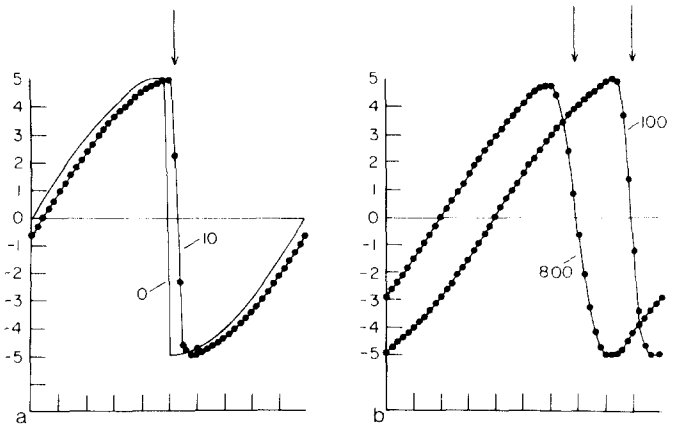

FIG. 4. Propagation of a sine wave interrupted by a discontinuity according to Eq. (1) for $\varepsilon = v\Delta t/\Delta x = 0.2$. Cubic interpolation, clipping and flux correction were implemented. The arrows indicate the position of the discontinuity in the analytic solution. (a) Solution after 0 and 10 time steps, (b) after 100 and 800 time steps.

extremum between u_j^n and u_{j-1}^n. The discontinuity is located exactly where it should be, according to the analytic solution (4).

In some applications exact flux conservation is not essential and it might suffice to incorporate only the propagation and the clipping states into a given code. Experiments with the square wave and sine wave worked well; however, the flanks diffused somewhat more than with flux correction. Runs with the cubic interpolation alone without clipping and redistribution produced over- and undershooting of at most 12%, which reduced to 4% after 800 time steps. This is shown in Figs. 5a, b, c for the square wave. Figure 6a, b shows the corresponding results for the sine wave with discontinuity.

To demonstrate the method we integrated the hydrodynamic equations (35) which are of form (19) for the isentropic case. The energy equation can be replaced by the entropy equation

$$\frac{\partial s}{\partial t} + u\frac{\partial s}{\partial x} = 0 \tag{8}$$

and the equations can be rewritten in terms of the Riemann invariants α and β [15] as

$$\begin{aligned} \frac{\partial \alpha}{\partial t} + (a + c)\frac{\partial \alpha}{\partial x} &= 0, \\ \frac{\partial \beta}{\partial t} + (a - c)\frac{\partial \beta}{\partial x} &= 0, \end{aligned} \tag{9}$$

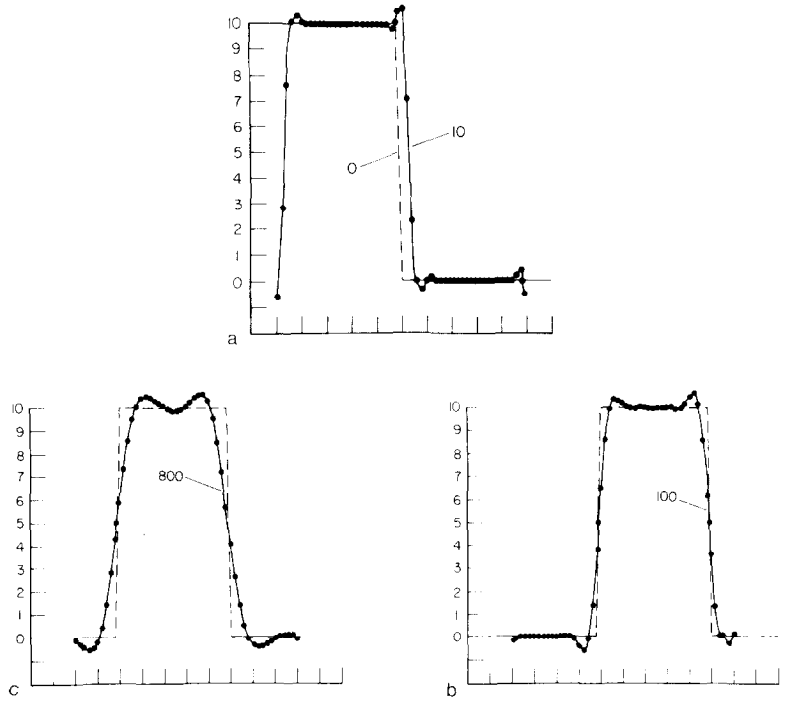

FIG. 5. Same as Fig. 3, but implementing only the cubic interpolation. There is overshooting near the shocks which spreads very slowly.

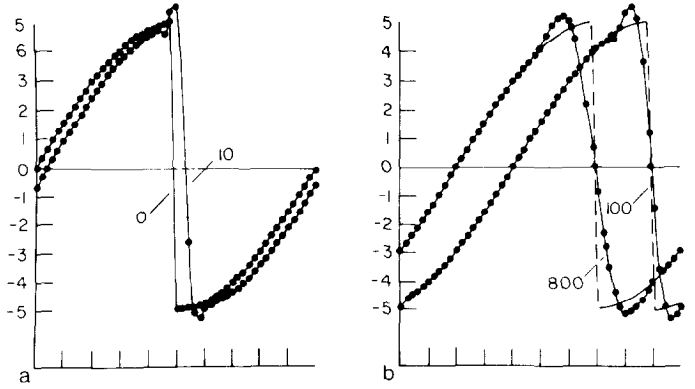

FIG. 6. Same as Fig. 4, but implementing only the cubic interpolation. There is a slight growth of the amplitude due to the nonmonotonicity.

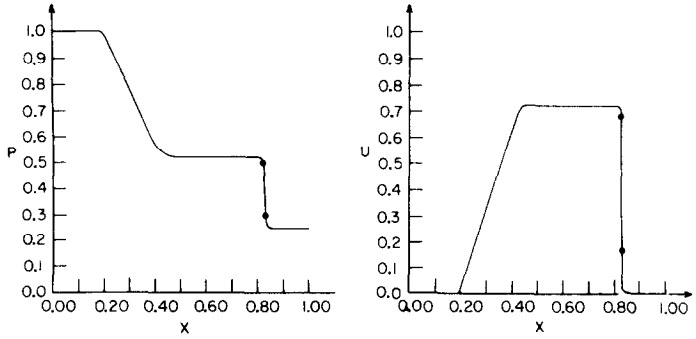

FIG. 7. The solution of an isentropic flow as described in Eqs. (9) and (10) after 40 time steps. Dots were drawn only in the shock region.

where

$$a = \tfrac{1}{2}(\alpha - \beta),$$
$$c = \tfrac{1}{4}(\gamma - 1)(\alpha - \beta). \tag{10}$$

Equations (9) and (10) are of the form (4) with the variable a being a function of α and β because of (10). The results are shown in Fig. 7. The shock is very steep and is represented by one to two zones only.

3. Conservative Equations

Equations of type (1) are very special in that their set of values $u(x, t)$ does not change in time. In general, however, the set of values $u(x, t)$ does change in time and then a direct application of the monotonicity principle as in Section 2 is no longer possible.

Before discussing a modified application of the monotonicity principle, we ask how we can construct in general numerical schemes which are second order in Δt. We first consider the system

$$\frac{\partial}{\partial t}\mathbf{u} = \mathbf{G}\mathbf{u}, \tag{11}$$

where $\mathbf{G}$ is a linear matrix operator independent of t, and $\mathbf{u}$ is a vector.

The solution is given by

$$\mathbf{u}(t + \Delta t) = \exp(\Delta t \mathbf{G})\,\mathbf{u}(t), \tag{12}$$

where the operator $\exp(\Delta t\,\mathbf{G})$ is defined by its Taylor series

$$\exp(\Delta t\,\mathbf{G}) = 1 + \Delta t\,\mathbf{G} + \tfrac{1}{2}(\Delta t)^2\,\mathbf{G}\cdot\mathbf{G} + O[(\Delta t)^3]. \tag{13}$$

We suggest the following method, which consists of two first order iterations of Eq. (11):

$$\mathbf{u}^* = \boldsymbol{u}^n + \Delta t\, \boldsymbol{G}\mathbf{u}^n, \tag{14}$$

$$\mathbf{u}^{**} = u^* + \Delta t\, \mathbf{G}u^*. \tag{15}$$

We assume that the last terms in (14) and (15) are calcuated with an error $O[(\Delta x)^3]$ or less in order to maintain overall second order accuracy. Then a second order solution is given by

$$\mathbf{u}^{n+1} = \tfrac{1}{2}(\mathbf{u}^n + \mathbf{u}^{**}). \tag{16}$$

The proof follows immediately if one inserts (15) and (14) into (16):

$$\mathbf{u}^{n+1} = \mathbf{u}^n + \Delta t\, \boldsymbol{G}\mathbf{u}^n + \tfrac{1}{2}(\Delta t)^2\, \mathbf{G} \cdot \mathbf{G}u^n. \tag{17}$$

If we expand u^{n+1} in powers of Δt,

$$\mathbf{u}^{n+1} = u^n + \Delta t \frac{\partial}{\partial t}\mathbf{u}^n + \frac{1}{2}\frac{\partial^2}{\partial t}u^n, \tag{18}$$

and make use of the original differential equation (11), it becomes obvious that the right-hand sides of (17) and (18) agree up to second order.

This method can be generalized to higher orders. For example, we can iterate once more,

$$u^{***} = u^{**} + \Delta t\, Gu^{**},$$

and obtain a third order solution given by

$$\mathbf{u}^{n+1} = \tfrac{1}{6}(2\mathbf{u}^n + 3\mathbf{u}^* + \mathbf{u}^{***}).$$

The iteration method works also for nonlinear equations. Let $\mathbf{G}$ be a nonlinear operator in conservation form, $\mathbf{G}u = \partial/\partial x\, \mathbf{F}(\mathbf{u})$. Then (11) becomes

$$\frac{\partial}{\partial t}\mathbf{u} = \frac{\partial}{\partial x}\mathbf{F}(\mathbf{u}). \tag{19}$$

The operator $\mathbf{F}$ does not depend explicitly on t or on derivatives of $\mathbf{u}$.

The iterated first order solutions are

$$\mathbf{u}^* = u^n + \Delta t \frac{\partial}{\partial x} F(\mathbf{u}^n), \tag{20}$$

$$\mathbf{u}^{**} = \mathbf{u}^* + \Delta t \frac{\partial}{\partial x}\mathbf{F}(u^*); \tag{21}$$

then the second order solution is again given by

$$u^{n+1} = \tfrac{1}{2}(\mathbf{u}^n + \mathbf{u}^{**}). \tag{22}$$

In both cases, expanding (22) and $\mathbf{u}(t + \Delta t)$ results in

$$u(t+\Delta t) = \mathbf{u}^n + \Delta t \frac{\partial}{\partial x} F(\mathbf{u}^n) + \frac{1}{2}(\Delta t)^2 \frac{\partial}{\partial x}\left[\left(\frac{\partial}{\partial x} F(u^n)\right) \frac{\partial}{\partial \mathbf{u}} F(\mathbf{u}^n)\right] + \cdots,$$

which proves the second order accuracy of (22) for the nonlinear equation (19).

So far we simply assumed that spatial derivatives are somehow taken care of by a finite difference approximation. We specify this now by

$$\left[\frac{\partial}{\partial x}\mathbf{F}(\mathbf{u})\right]_{j+1/2} = (F_{j+1} - F_j)/\Delta x + O[(\Delta x)2], \tag{23}$$

which introduces a half-integer mesh, similar to the Lax–Wendroff scheme.

The first terms on the right side of (20) and (21) are approximated by

$$u_{j+1/2} = \tfrac{1}{2}(\mathbf{u}_{j+1} + \mathbf{u}_j) - \tfrac{1}{16}(\delta^2 \mathbf{u}_{j+1} + \delta^2 \mathbf{u}_j) + O[(\Delta x)^4]. \tag{24}$$

We summarize Eqs. (20) to (24) for easy reference:

$$\begin{aligned} u^*_{j+1/2} &= \frac{1}{2}(u^n_{j+1} + u^n_j) - \frac{1}{16}(\delta^2 u_{j+1} + \delta^2 u_j) + \frac{\Delta t}{\Delta x}(F^n_{j+1} - F^n_j), \\ u^{**}_j &= \tfrac{1}{2}(u^*_{j+1/2} + u^*_{j-1/2}) - \tfrac{1}{16}(\delta^2 u^*_{j+1/2} + \delta^2 u^*_{j-1/2}) \\ &\quad + \frac{\Delta t}{\Delta x}(F^*_{j+1/2} - F^*_{j-1/2}), \\ u^{n+1}_j &= \tfrac{1}{2}(u_j + u^{**}_j). \end{aligned} \tag{25}$$

We still have to show that (25) is stable. This is difficult to show for the general case, but it can easily be done for the linear equation (4). With a standard mode analysis, we obtain, from (25),

$$\begin{aligned} u^* &= u \exp(i\kappa/2)\, R, \\ u^{**} &= u^* \exp(-i\kappa/2)\, R \end{aligned} \tag{26}$$

with

$$R = \cos\kappa/2\,(1 + \tfrac{1}{2}\sin^2\kappa/2) - 2i\xi \sin\kappa/2, \tag{27}$$

where $\kappa = k \cdot \Delta x$, k is the wave number and $\xi = \Delta t\, a//\Delta x$. The amplification factor M is given, according to (25), by

$$\begin{aligned} M &= n^{n+1}/u^n = \tfrac{1}{2}(1 + R^2) \\ &= 1 + \cos^2 \kappa/2(1 + \tfrac{1}{2}\sin 2\kappa/2)^2 - 4\xi^2 \sin^2 \kappa/2 \\ &\quad - 2i\xi \sin \kappa(1 + \tfrac{1}{2}\sin^2 \kappa/2). \end{aligned} \tag{28}$$

Expansion in powers of κ gives

$$|M|^2 = 1 - \tfrac{1}{4}(\kappa/2)^4 (3 - 16\xi^4). \tag{29}$$

Usually the most unstable mode is $\kappa = \pi$. This value, inserted into (28), gives a stability criterion

$$|\xi| \leqslant \tfrac{1}{2}, \tag{30}$$

which is more stringent than the one derived from (29).

4. Discontinuities

In the neighborhood of discontinuities the second order system (25) gives unsatisfactory results and we have to ask how the scheme can be modified near a discontinuity or shock and how the code can automatically diagnose such irregularities.

If the solution is regular, the interpolated value (24) for $u_{j+1/2}$ should lie between u_{j+1} and u_j, with the only exception being extrema in that interval. However, if the condition

$$\mathrm{Min}(u_{j+1}, u_j) \leqslant u_{j+1/2} \leqslant \mathrm{Max}(u_{j+1}, u_j) \tag{31}$$

is violated, we enforce it by replacing (24) by

$$u_{j+1/} = \tfrac{1}{2}(u_{j+1} + u_j), \tag{32}$$

which satisfies monotonicity trivially. In other words: given a set of points u_j on an integer mesh, we produce another set of points $u_{j+1/2}$ on an half-integer mesh by applying (24). If monotonicity is violated, we enforce it by substituting (32) for (24) pointwise. Contrary to the procedure in Section 2, we do not have to know any properties of the differential equation to apply the monotonicity principle. The principle is being used in a purely geometrical context. As a consequence, it does not prevent new extrema in the solution of a differential equation. It even does not prevent over- or undershooting of the solution, but it should have a smoothing effect. The replacement of (24) by (32) can also be interpreted as adding a diffusive term $1/16(\delta^2 u_{j+1} + \delta^2 u_j)$ to the first order solutions of (19) to the regions where overshooting occurs.

Equations (32) and (24), when linearized, are related to Boris and Book's scheme SHASTA [4]. However, we aply this formula only pointwise, where the equations are strongly nonlinear, whereas Boris and Book apply it to all points.

Substituting (32) for (24) violates the conservation property of (19). We made use of two different ways to keep the system conservative. First, we write the first equation of Eq. (25) as

$$u^*_{j+1/2} = \tfrac{1}{2}(u^n_{j+1} + u^n_j) - \frac{\Delta t}{\Delta x}(F^n_{j+1} - F^n_j) + g_{j+1} - g_j \tag{33}$$

with

$$g_j = -\tfrac{1}{16}(u_{j+1} - u_{j-1})$$

and the second equation correspondingly. By replacing g_{j+1} by g_j or g_j by g_{j+1} we can easily substitute (32) for (24) and conserve flux at the same time.

If

$$|\delta^2 u_{j+1}| > |\delta^2 u_j| \qquad \text{we put} \qquad g_{j+1} = g_j \tag{34}$$

but if

$$|\delta^2 u_{j+1}| < |\delta^2 u_j| \qquad \text{we put} \qquad g_j = g_{j+1}.$$

With this choice, we intend to shift the "clippings," i.e., the difference between values (24) and (32) toward the discontinuity. Many other choices different from (34) are possible.

If our computational loop goes from left to right, the replacement of g_{j+1} by g_j will be checked for consistency automatically later in the loop. However, if g_j is replaced by g_{j+1}, we might have created some overshooting in $u_{j-1/2}$ which remains uncorrected. Thus the arbitrary choice of running a computation loop from left to right might introduce asymmetries in the solution.

The second method of flux conservation was described in Section 2, namely that the "clippings" are distributed to adjacent mesh points.

In one variation 50% of the clippings were distributed to the right, 50% to the left. If this created overshooting, only so much was added to $u_{j+1/2\pm 2}$ as to not create overshooting. This procedure was repeated with points $u_{j+1/2+2}$ if necessary. If clippings were left over they were simply neglected. In principle this procedure did not preserve the flux exactly. In practice, however, little difference was seen when this scheme was compared with other distribution schemes in which the flux was exactly conserved.

Runs made with the square wave test showed that the first method, adjusting the g_j's, was slightly more diffusive than the second method, which distributed the clippings. We therefore present an integration of the one-dimensional hydrodynamic equations for the clipping method only, following Sod [13] closely.

The equations are exactly in form (19) with

$$\mathbf{u} = \begin{pmatrix} \rho \\ m \\ e \end{pmatrix}; \qquad \mathbf{F}(\mathbf{u}) = -\begin{pmatrix} m \\ m^2/\rho + p \\ m/\rho(e + p) \end{pmatrix}, \tag{35}$$

where ρ is the density, $m = \rho \mathbf{u}$ is momentum, e is energy per unit volume. We assume a polytrophic gas for which $p = A(s)\rho^{\gamma}$, where s is the entropy. In terms of the energy we have

$$p = (\gamma - 1)(e - \tfrac{1}{2}m^2/\rho),$$

where we put the ratio of specific heats, $\gamma = 1.4$. The initial conditions are the same as Sod's. The results are shown in Fig. 8 after 80 time steps. The shock in density,

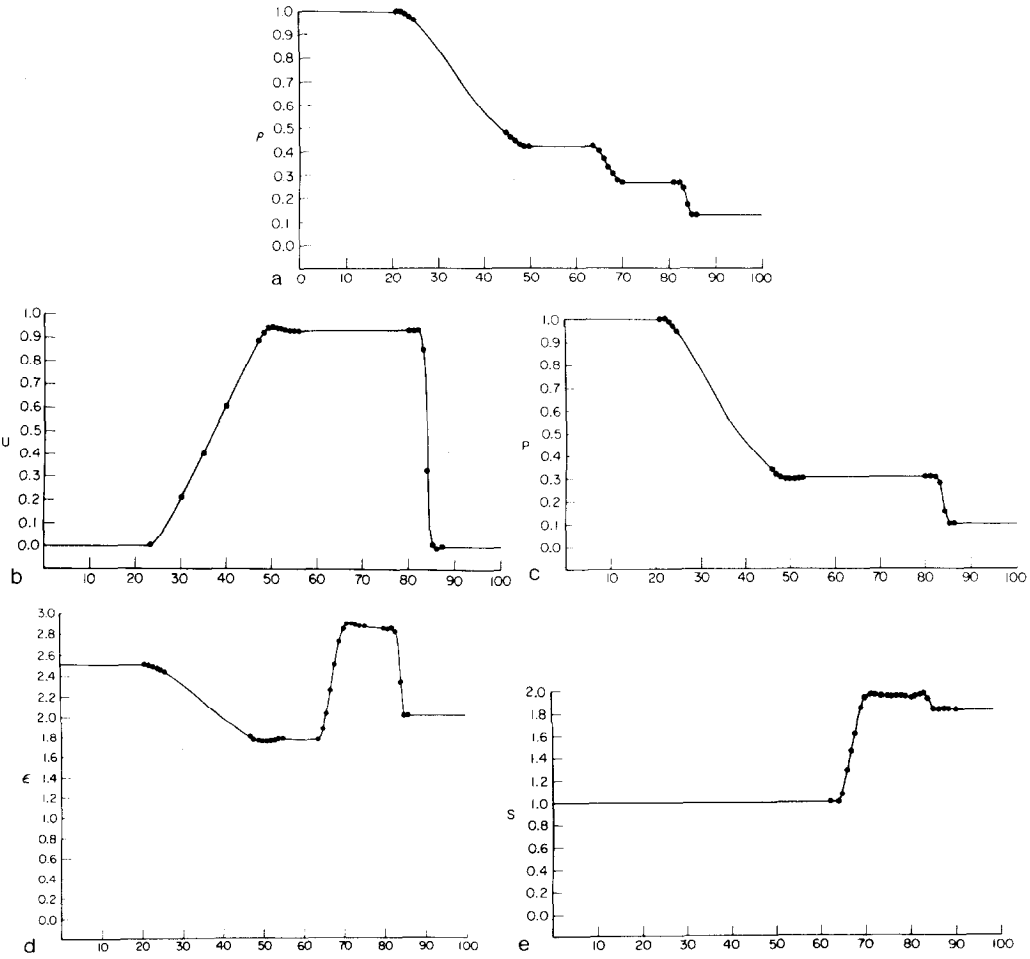

FIG. 8. Solution of the Riemann problem in one dimension. (a) Density ρ, (b) velocity u, (c) pressure p, (d) energy ε, (e) entropy s.

velocity, pressure and energy occupies two to three zones. The contact discontinuity in the density and energy has spread to a thickness of five zones. The density plateau between shock and contact discontinuity is well represented. In the velocity and pressure profiles small overshootings of about 1% can be observed at the right onset of the rarefaction wave. The corners of the rarefaction are only slightly rounded.

5. Conclusions

We applied the monotonicity principle to convective equations and to flux conserving partial differential equations. In the first case the monotonicity was a consequence of a property of the differential equation. Flux conservation was enforced by distributing surplus flux to neighboring mesh points.

In the second case the monotonicity requirement was used as an additional requirement when interpolating a given set of points representing a physical variable which can contain a discontinuity. Violation of the monotonicity was diagnosed as the occurrence of a discontinuity and the higher order integration scheme was replaced by a diffusive lower order scheme. The number of possible implementations is very large and we have experimented with only a small fraction of it. In this sense the method contains many parameters. However, these parameters are independent of a given problem, in contrast to some of the methods discussed by Sod.

Our method is easily implemented and should not require much more computation time than an uncorrected procedure. The monotonicity has to be checked for each variable at every mesh point and time step once or twice. As most of the points lie in smooth regions of the curve, nothing more must be done. Only at shocks or discontinuities need the flux be redistributed or adjusted.

The generalization of the method to two dimensions has not been tested yet. It appears that the formulae become more diffusive, but apart from that we do not anticipate major problems.

Acknowledgments

We are greatful to Dr. D. L. Book, who reviewed an earlier version this paper. This work was supported in part by U.S. Department of energy Grant EY–76–S–02–2059.

References

1. R. D. Richtmyer and K. W. Morton, "Difference Methods for Initial-Value Problems," Chap. 12, Interscience, New York, 1967.
2. P. F. Roache, "Computational Fluid Dynamics," Chap. 5, Hermosa, Albuquerque, 1972.
3. A. C. Vliegenhart, *J. Eng. Math.* **4** (1970), 341.
4. J. P. Boris and D. L. Book, *J. Comput. Phys.* **11** (1973), 38.
5. D. L. Book, J. P. Boris, and K. H. Hain, *J. Comput. Phys.* **18** (1975), 248.
6. J. P. Boris and D. L. Book, *J. Comput. Phys.* **20** (1976), 397.

7. J. P. BORIS AND D. L. BOOK, *in* "Methods in Computational Physics" (J. Killeen, Ed.), Vol. 16, p. 85, Academic Press, New York, 1976.
8. A. HARTEN, *Commun. Pure Appl. Math.* **30** (1977), 611.
9. A. HARTEN, *Math. Comput.* **32** (1978), 363.
10. B. VAN LEER, *in* "Proceedings, 3rd Int. Conf. Num. Math. in Fluid Mechanics, July 1972," p. 163, Lecture Notes in Physics No. 18, Springer-Verlag, New York/Berlin, 1973.
11. B. VAN LEER, *J. Comput. Phys.* **14** (1974), 161.
12. B. VAN LEER, *J. Comput. Phys.* **23** (1977), 276.
13. G. H. SOD, *J. Comput. Phys.* **27** (1978), 1.
14. C. Z. CHENG AND G. KNORR, *J. Comput. Phys.* **22** (1976), 330.
15. R. COURANT AND K. O. FRIEDRICHS, "Supersonic Flow and Shock Waves," paragraph 37, Interscience, New York, 1948.